



UNIVERSITY OF LEEDS

This is a repository copy of *Epitaxial Bi 9 Ti 3 Fe 5 O 27 thin films: a new type of layer-structure room-temperature multiferroic*.

White Rose Research Online URL for this paper:  
<http://eprints.whiterose.ac.uk/120729/>

Version: Accepted Version

---

**Article:**

Cao, X, Liu, Z, Dedon, LR et al. (6 more authors) (2017) Epitaxial Bi 9 Ti 3 Fe 5 O 27 thin films: a new type of layer-structure room-temperature multiferroic. *Journal of Materials Chemistry C*, 5 (31). pp. 7720-7725. ISSN 2050-7526

<https://doi.org/10.1039/C7TC02666H>

---

© 2017, The Royal Society of Chemistry. This is an author produced version of a paper published in *Journal of Materials Chemistry C*. Uploaded in accordance with the publisher's self-archiving policy.

**Reuse**

Items deposited in White Rose Research Online are protected by copyright, with all rights reserved unless indicated otherwise. They may be downloaded and/or printed for private study, or other acts as permitted by national copyright laws. The publisher or other rights holders may allow further reproduction and re-use of the full text version. This is indicated by the licence information on the White Rose Research Online record for the item.

**Takedown**

If you consider content in White Rose Research Online to be in breach of UK law, please notify us by emailing [eprints@whiterose.ac.uk](mailto:eprints@whiterose.ac.uk) including the URL of the record and the reason for the withdrawal request.



[eprints@whiterose.ac.uk](mailto:eprints@whiterose.ac.uk)  
<https://eprints.whiterose.ac.uk/>

# Epitaxial Bi<sub>9</sub>Ti<sub>3</sub>Fe<sub>5</sub>O<sub>27</sub> Thin Films: A New Type of Layer-Structure

## Room-Temperature Multiferroic

Xun Cao,<sup>a,b\*</sup> Zhiqi Liu,<sup>c</sup> Liv R Dedon,<sup>b</sup> Andrew J Bell,<sup>d</sup> Faye Esat,<sup>d</sup> Yujia Wang,<sup>e</sup> PuYu,<sup>e</sup> Chuanshou Wang,<sup>f</sup> and Ping Jin<sup>a,g</sup>

<sup>a</sup> State Key Laboratory of High Performance Ceramics and Superfine Microstructure, Shanghai Institute of Ceramics, Chinese Academy of Sciences, Dingxi 1295, Changning, Shanghai, 200050, China.

<sup>b</sup> Department of Materials Science and Engineering, University of California Berkeley, Berkeley, CA 94720, U.S.A

<sup>c</sup> School of Materials Science and Engineering, Beihang University, Beijing, 100191, China

<sup>d</sup> School of Chemical and Process Engineering, University of Leeds, Leeds, LS2 9JT, U.K

<sup>e</sup> Department of Physics, Tsinghua University, Beijing, 100084, China.

<sup>f</sup> Department of Physics, Beijing Normal University, Beijing, 100875, China.

<sup>g</sup> Materials Research Institute for Sustainable Development, National Institute of Advanced Industrial Science and Technology, Nagoya 463-8560, Japan

\*

### Corresponding authors:

Dr. Xun Cao

State Key Laboratory of High Performance Ceramics and Superfine Microstructure, Shanghai Institute of Ceramics, Chinese Academy of Sciences, Shanghai 200050, China

E-mail: (X. Cao)[caoxun2015@gmail.com](mailto:caoxun2015@gmail.com) Tel.: +86 21 6990

6206.

Fax: +86 21 6990 6221.

## **Abstract**

In this letter, we report the successful growth of high-quality Aurivillius oxide thin films with  $m = 8$  ( $m$  denotes the period of the Aurivillius structure) using pulsed laser deposition. Both ferroelectric and magnetic properties of the layer-structure epitaxial  $\text{Bi}_9\text{Ti}_3\text{Fe}_5\text{O}_{27}$  films were investigated. Surprisingly, the optimized thin films exhibit in-plane ferroelectric polarization switching as well as ferromagnetism even at room temperature, though the bulk material is antiferromagnetic. In addition, dielectric measurements indicate that such thin films exhibit potential for high-frequency device applications. This work therefore demonstrates a new pathway to developing single-phase multiferroic materials where ferroelectricity and ferromagnetism coexist with great potential for low energy device applications.

## Introduction

There has been a long-standing challenge in the fabrication of epitaxial thin films of layered Aurivillius oxides due to their thermodynamic phase-instability and the large stacking layer number.<sup>1</sup> However, the demand for high-quality thin films has been strongly increased by their promising room-temperature multiferroic properties.<sup>2</sup> Single-phase multiferroic thin films are favorable for device applications because of their potential for realizing cross-control between ferroelectric and ferromagnetic orders in low energy and highly integrated devices.<sup>3,4</sup> The  $\text{Bi}_4\text{Ti}_3\text{O}_{12}\text{-BiFeO}_3$  system is known to contain a series of compounds with the general formula  $\text{Bi}_{m+1}\text{Fe}_{m-3}\text{Ti}_3\text{O}_{3m+3}$ .<sup>5-7</sup> These compounds possess layered perovskite-like structures, first described by Aurivillius, in which fluorite-like bismuth-oxygen layers of composition  $\{(\text{Bi}_2\text{O}_2)^{2+}\}$  alternate with (001) perovskite-like slabs of composition  $\{(\text{Bi}_{m+1}\text{Fe}_{m-3}\text{Ti}_3\text{O}_{3m+1})^{2-}\}$ .<sup>8</sup> Fractional  $m$  values correspond to mixed-layer structures, which contain perovskite-like slabs of different thicknesses.

The compound  $\text{Bi}_9\text{Ti}_3\text{Fe}_5\text{O}_{27}$  (BTFO) has eight perovskite layers between the  $\text{Bi}_2\text{O}_2$  layers. The scientific and practical application value of BTFO arises from its multiferroic properties – namely ferroelectric and antiferromagnetic – which are simultaneously exhibited in bulk.<sup>9</sup> The antiferromagnetic Neel temperature  $T_N$  of bulk BTFO has not been precisely determined. Instead, the value of  $T_N$  is estimated to be as high as 360 K, above which the compound transitions to a paramagnetic state.<sup>10</sup> Coherent intergrowths of structural elements rather similar to tetragonal-tungsten-bronze-type were observed and these sometimes appeared to be relics of the super-lattice phase.<sup>11</sup>

The vast majority of previous studies have mainly focused on bulk BTFO compounds.<sup>9,11,12</sup> Until now, very little work has been done on BTFO thin films, due to the difficulty in fabricating high-quality epitaxial single-crystalline thin films. The layered structures and complicated compositions have posed significant challenges to film growth. In the similar Ruddlesden-Popper series, theoretical calculations have shown that the thermal-equilibrium energies of various phases with different numbers of layers approach a constant value when  $m$  is larger than 3,<sup>13</sup> which causes experimentally observed intergrowths during the synthesis of bulk compounds.<sup>14,15</sup> Similar phenomena have occurred during the synthesis of bulk Aurivillius compounds as well.<sup>15,16</sup> To achieve high-quality single-crystalline films in this work, we employed pulsed laser deposition,

which can be a superior method for growing highly epitaxial complex oxides that are unstable in bulk. In this work, c-axis-oriented BTFO epitaxial thin films were successfully fabricated with uniform  $m = 8$  Aurivillius structures by optimizing growth parameters, namely the growth temperature and oxygen pressure. More importantly, lattice-matched substrates were chosen to achieve strained and high-quality epitaxial films, which are crucial for stabilizing a novel ferromagnetic phase in our thin films.

## Experimental

BTFO thin films and SrRuO<sub>3</sub>(SRO)/BTFO heterostructures were grown on TiO<sub>2</sub>-terminated SrTiO<sub>3</sub> (STO) (001) substrates using pulsed laser deposition with a KrF excimer laser ( $\lambda=248$  nm). All substrates had a vicinal angle of  $\sim 0.1^\circ$ . BTFO targets with about 10% excess Bi and stoichiometric SRO targets were ablated at a laser fluency of  $\sim 1.2$  J/cm<sup>2</sup> and a repetition rate of 17 Hz and 5Hz for the growth of SRO and BTFO, respectively. During the BTFO growth, the STO substrates were held at 700°C in a dynamic oxygen pressure of 100 mTorr. For the SRO layer growth, the temperature was 650°C. After growth, as-grown BTFO films and heterostructures were cooled to room temperature at a rate of  $\sim 5$  °C/min in 760 Torr of oxygen to optimize oxidation. The film structure was studied by high-resolution X-ray diffraction (HRXRD) (PANalytical, X'Pert PRO) and scanning transmission electron microscopy (STEM). Film morphology and ferroelectric domain structure were investigated using atomic force microscopy (AFM) and piezoelectric force microscopy (PFM) (Bruker, Dimension Icon & Multimode 8) with commercially available TiPt-coated Si tips (Mikro Masch) with a tip curvature radius of  $\sim 30$  nm. All the AFM and PFM tests were carried out at room temperature. A superconducting quantum interference device (SQUID) (Quantum Design) was used to examine the magnetic properties of the films with the magnetic field applied parallel to the thin film plane. Dielectric and electrical characterization was performed using an E4980 LCR meter (Agilent) and 6517B electrometer (Keithley/Tektronix).

## Results and Discussion

**Figure 1(a)** shows the X-ray diffraction (XRD)  $\omega$ - $2\theta$  scans of BTFO/STO (001) and BTFO/SRO/STO heterostructures. The diffraction peaks demonstrate an  $m = 8$  Aurivillius structure with a similar c axis lattice constant with or without the SRO bottom electrode. No other peaks were found showing that the BTFO epitaxial films are single-phase. The thickness fringes

of the main peaks (0012) and (0024) in **Figure 1(b)** indicate the high-quality coherent growth of interlayers in the as-grown epitaxial BTFO films. The observation of the layer thickness fringes also indicates that the top surface is smooth and the interface between the layered structures is abrupt.<sup>17</sup> The high-resolution AFM image (left panel of **Figure 1(c)**) indicates step-flow growth of the layered-perovskite BTFO films with a surface step height of  $\sim 3.8$  nm (half of the BTFO unit cell) as seen in the height profile on the right panel of **Figure 1(c)**. The bulk lattice constants are  $a = 5.536$  Å,  $b = 5.602$  Å and  $c = 75.16$  Å, respectively.<sup>7,9</sup> In order to confirm the surface roughness of the SRO bottom layer, the root-mean-square roughness (RMS) of a 30 nm SRO film grown on STO (**Figure 1(d)**) was of the order of the pseudocubic unit cell (RMS = 0.136 nm), and the terraces due to the  $< 0.5^\circ$  miscut of the STO substrate were clearly seen at the surface of the film. The X-ray reciprocal space mapping was employed to determine the strain state of the as-grown films. The BTFO films and the SRO bottom layer are found to be coherently strained to the STO substrate, as shown in **Figure 1(e)**. This can be easily understood since BTFO can sit on the SRO/STO unit cell with the following relation:  $a_{\text{BTFO}}(5.536 \text{ \AA}) \approx a_{\text{SRO}}(5.543 \text{ \AA}) \approx a_{\text{STO}}(5.52 \text{ \AA})$ .<sup>18,19</sup>

The cross-section atomic structure of an as-grown BTFO film with a SRO bottom electrode layer was measured with aberration-corrected STEM high-angle annular dark-field (STEM HAADF), as shown in **Figure 2**. **Figure 2(a)** illustrates a schematic of the BTFO layered perovskite structure with  $m = 8$ . As seen in the TEM images, the BTFO film exhibits a uniform  $m = 8$  structure within the entire measured thickness range, as there were seven layers of perovskite sandwiched by two closely stacked  $\text{Bi}_2\text{O}_2$  bilayer. The thickness of the bottom electrode SRO film and the BTFO film is  $20 \pm 0.5$  and  $55 \pm 0.7$  nm, respectively, as shown in **Figure 2(b)**. **Figure 2(c)** shows a high-resolution image of the layer-structured BTFO film. Some stacking faults can be observed in  $(\text{Bi}_2\text{O}_2)^{2-}$  bilayer. The c-axis lattice parameter determined from high-resolution STEM images is  $7.58 \pm 0.15$  nm, which is in good agreement with the XRD results and that of bulk compound.<sup>9</sup> The interface between the STO substrate and SRO as well as the interface between SRO and BTFO are shown in **Figures 2(d)&(e)**, respectively. The STEM images overall illustrate the high epitaxial quality of BTFO and SRO films on the STO substrate.

As illustrated in **Figure 3**, a conductive epitaxial SRO layer was used as bottom contact in the BTFO/SRO/STO heterostructure during nanoscale probe bias control. For the 20 V probe bias poling of the BTFO/SRO/STO heterostructure, the in-plane domain switching is clear while the

out-of-plane domain switching is not visible before and after the application of an electric field, as shown in **Figure 3(b)&(d)**. This illustrates that the polarization of BTFO films should be mainly in-plane. It is reported that in  $\text{Bi}_4\text{Ti}_3\text{O}_{12}$  single crystals, the spontaneous polarization shows a large component along the  $a$  axis and a smaller component along the  $c$  axis.<sup>20</sup> So it is reasonable to assume that the spontaneous polarization of BTFO lies in-plane. In an approximately 55 nm thick BTFO thin film, the in-plane ferroelectric polarization was switched under the application of a probe bias of approximately +20 V as shown in **Figure 3(b)**. Detailed domain structure imaging should be conducted in order to reveal the anisotropic ferroelectric switching in BTFO films.

The magnetic properties of epitaxial BTFO films were measured with BTFO/STO heterostructures using a SQUID magnetometer. **Figure 4(a)** shows in-plane magnetization curves as a function of magnetic field ( $M$ - $H$ ) at different temperatures after subtracting the diamagnetic signal of the STO substrate. Surprisingly, the heterostructures exhibit obvious hysteresis loops with clear saturation, characteristics of ferromagnetism. The ferromagnetism persists from 2K to 300K, and the saturation magnetization  $M_s$  decreases from 10.3 to 7.8  $\text{emu}/\text{cm}^3$  during heating. This is, to our best knowledge, the first report of clear ferromagnetism for the 8 layer BTFO Aurivillius structure, which is antiferromagnetic in bulk.

Furthermore, the coercive field and remnant magnetization can be seen in the inset of **Figure 4(a)**. With increasing temperature, the coercive field decreases from 176.9 to 39.3 Oe and the remnant magnetization ( $M_r$ ) decreases from 3.29 to 0.76  $\text{emu}/\text{cm}^3$ . The strong temperature dependence of saturation magnetization, remnant magnetization, and coercive field are well in contrast to the temperature dependence of high-temperature ferromagnetic impurities such as Fe clusters, confirming the intrinsic ferromagnetic order in the epitaxial thin films.

It is clear that all the remnant magnetization ratios  $M_r/M_s$  are less than 1 for all temperatures, which indicates that the easy axis the magnetization is not well confined in-plane but likely canted out-of-plane. This is reminiscent of the novel ferromagnetism in antiferromagnetic  $\text{BiFeO}_3$  thin films, where the ferromagnetism emerges as a result strain-enhance asymmetric Dzyaloshinskii-Moriya (DM) exchange interaction in non-collinear and frustrated spin systems or competition between magnetic surface anisotropy and shape anisotropy.<sup>21</sup> In our case, epitaxial BTFO films are coherently strained to the STO substrate, with the in-plane lattice constant  $a = 5.52 \text{ \AA}$ , corresponding to 0.3% compressive strain compared with the bulk lattice  $a = 5.536 \text{ \AA}$ . More

importantly, bulk BTFO has an orthorhombic symmetry while BFTO thin films are tetragonal due to the coherent epitaxial strain. The modification of the strain state and the lattice symmetry via epitaxy in single-crystal films can definitely influence the magnetic exchange interaction among Fe ions, leading to large enhancement of the ferromagnetic order in an antiferromagnetic matrix in epitaxial BTFO films.<sup>22</sup>

To further investigate the nature of the ferromagnetic interaction in the epitaxial BTFO films, temperature dependence of both zero-field-cooled (ZFC) and field-cooled (FC) magnetization were measured under an in-plane magnetic field of 1000 Oe with a cooling field of 1000 Oe for FC measurements. The bifurcation between ZFC and FC curves below 250 K [**Figure 4(b)**] highlights the existence of spin frustration in the ferromagnetic system. Upon cooling under a magnetic field, the spin frustration is, to some extent, suppressed, while ferromagnetic domains grow and increasingly interact with one another. As a consequence, the FC magnetization is larger than the ZFC magnetization. In addition, magnetic properties of strongly correlated systems are rather sensitive to spin arrangements<sup>23,24</sup> and the repeatable anomaly in the M-T curves around 250K may imply a spin re-orientation in BFTO films.

The electrical and dielectric properties of BTFO films were also investigated. Symmetric circular capacitor structures with diameters ranging from 5 to 40  $\mu\text{m}$  were fabricated by ex situ deposition of 80 nm thick SRO top electrodes defined using a MgO hard-mask process, as shown in the inset of **Figure 5(a)**.<sup>25,26</sup> As shown in **Figure 5(a)**, the current-voltage curves are highly symmetric and exhibit very low leakage current. **Figure 5(b)** shows the frequency dependence of the dielectric constant ( $\epsilon$ ) and the loss tangent ( $\tan \delta$ ) in BTFO thin films. Both the  $\epsilon$  and  $\tan \delta$  are stable at the high frequency region from 10 KHz to 1 MHz, implying great potential in high-k dielectric applications.

## Conclusion

In summary, we have successfully fabricated high-quality epitaxial BTFO films ( $m = 8$ ) on STO (001) substrates using pulsed laser deposition. HRXRD and HRTEM measurements confirm that the films exhibit a uniform  $m = 8$  layered structure and are coherently-strained to the STO (001) substrate even with a SRO bottom electrode layer. The clear in-plane ferroelectric domain switching with robust ferromagnetism at room temperature illustrate that this material is a new type of single-phase room-temperature multiferroic with coexistence of ferroelectricity and

ferromagnetism. This work therefore provides an attractive path of using epitaxial strain to realizing highly-desirable ferroelectric-ferromagnetic thin films for low energy multiferroic device applications.

## Notes

The authors declare no competing financial interest.

## Acknowledgements

This study was financially supported by the National Natural Science Foundation of China (NSFC, No.: 51572284), and the China Scholarship Council (CSC). The authors want to thank Ran Gao and Dr. Xiaoyan Lu from University of California, Berkeley, for their discussion of XRD and AFM test. The growth of the film was performed in University of California, Berkeley under the supervision of R. Ramesh.

Thanks to Prof. R. Ramesh of University of California, Berkeley.

## References

- (1) Yun Y.; Ma C.; Zhai X.; Huang H.; Meng D.; Wang J.; Fu Z.; Peng R.; Brown G. J.; Lu Y. Interface Engineering in Epitaxial Growth of Layered Oxides via a Conducting Layer Insertion. *Appl. Phys. Lett.* 2015, 107, 011602.
- (2) Ramesh R., Spaldin N.A.; Multiferroics: progress and prospects in thin films. *Nat. Mater.* 2007, 6 (1), 21-29.
- (3) Eerenstein W.; Mathur N. D.; Scott J. F. Multiferroic and Magnetoelectric Materials. *Nature* 2006, 442, 759-765.
- (4) Gajek M.; Bibes M.; Fusil S.; Bouzouane K.; Fontcuberta J.; Barthelemy A.; Fert A. Tunnel Junctions with Multiferroic Barriers. *Nat. Mater.* 2007, 6, 296-302.
- (5) Smolenskii G. A.; Isupov V. A.; Agranovskaya A. I. A New Group of Ferroelectrics (with Layered Structure): II, *Fiz. Tverd. Tela (Leningrad)* 1963, 3, 896-901.
- (6) Boullay P.; Trolliard G.; Mercurio D. Toward a Unified Approach to the Crystal Chemistry of Aurivillius-Type Compounds.: I. The Structural Model. *J. Solid State Chem.* 2002, 164, 252-260.
- (7) Lomanova N. A.; Morozov M. I.; Ugolkov V. L.; Gusarov V. V. Properties of Aurivillius Phases in the  $\text{Bi}_4\text{Ti}_3\text{O}_{12}$ - $\text{BiFeO}_3$  System. *Inorg. Mater.* 2006, 42, 189-195.

- (8) Aurivillius, B. Family of Layered Bismuth Compounds. *Ark. Kemi* 1949, 1, 463-480.
- (9) Mazurek M.; Jartych E.; Lisinska-Czekaj A.; Czekaj D.; Oleszak D. Structure and Hyperfine Interactions of  $\text{Bi}_9\text{Ti}_3\text{Fe}_5\text{O}_{27}$  Multiferroic Ceramic Prepared by Sintering and Mechanical Alloying Methods. *J. Non-Crys. Solid* 2010, 356, 1994-1997.
- (10) Srinivas A.; Kim D. W.; Hong K. S.; Suryanarayana S. V. Study of Magnetic and Magnetoelectric Measurements in Bismuth Iron Titanate Ceramic- $\text{Bi}_8\text{Fe}_4\text{Ti}_3\text{O}_{24}$ . *Mater. Res. Bull.* 2004, 39, 55-61.
- (11) Smith D. J.; Hutchison J. L. Intergrowths and Defect Structures in  $\text{Bi}_9\text{Ti}_3\text{Fe}_5\text{O}_{27}$  Revealed by High-Resolution Electron Microscopy. *J. Micro.* 1983, 129, 285-293.
- (12) Ismailzade I. H.; Yakupov R. G.; Melik-shanazarova T. A. The Magnetoelectric Effect in Ferroelectric-Antiferromagnetic  $\text{Bi}_5\text{Bi}_4\text{Ti}_3\text{Fe}_5\text{O}_{27}$ . *Phys. Stat. Sol. (a)* 1971, 6, K85-K87.
- (13) Bacq O. Le; Salinas E.; Pisch A.; Bernard C.; Pasturel A. First-Principles Structures Stability in the Strontium-Titanium-Oxygen System. *Philos. Mag.* 2006, 86, 2283-2292.
- (14) Tilley R. J. D. An Electron Microscope Study of Perovskite-Related Oxides in the  $\text{Sr}\square\text{Ti}\square\text{O}$  System. *J. Solid State Chem.* 1977, 21, 293-301.
- (15) Zurbuchen M. A.; Tian W.; Pan X. Q.; Fong D.; Streiffer S. K.; Hawley M. E.; Lettieri J.; Jia Y.; Asayama G.; Fulk S. J.; Comstock D. J.; Knapp S.; Carim A. H.; Schlom D. G. Morphology Structure, and Nucleation of Out-of-Phase Boundaries (OPBs) in Epitaxial Films of Layered Oxides. *J. Mater. Res.* 2007, 22, 1439-1471.
- (16) Zhou J.; Wu F. X.; Chen Y. B.; Zhang S. T.; Chen Y. F. Structural Stability of Layered  $n\text{-LaFeO}_3\text{-Bi}_4\text{Ti}_3\text{O}_{12}$ ,  $\text{BiFeO}_3\text{-Bi}_4\text{Ti}_3\text{O}_{12}$ , and  $\text{SrTiO}_3\text{-Bi}_4\text{Ti}_3\text{O}_{12}$  Thin Films. *J. Mater. Res.* 2012, 27, 2956-2964.
- (17) Larsson M. I.; Joelsson W. Ni, K.; Hansson G. V. Growth of High Quality Ge Films on Si (111) Using Sb as Surfactant. *Appl. Phys. Lett.* 1994, 65, 1409-1411.
- (18) Wu X. D.; Foltyn S. R.; Dye R. C.; Counter Y.; Muenchausen R. E. Properties of Epitaxial  $\text{SrRuO}_3$  Thin Films. *Appl. Phys. Lett.* 1993, 62, 2434-2436.
- (19) Kacedon D. B.; Rao R. A.; Eom C. B. Magnetoresistance of Epitaxial Thin Films of Ferromagnetic Metallic Oxide  $\text{SrRuO}_3$  with Different Domain Structures. *Appl. Phys. Lett.* 1997, 71, 1724-1726.
- (20) Cummins S. E.; Cross L. E. Electrical and Optical Properties of Ferroelectric  $\text{Bi}_4\text{Ti}_3\text{O}_{12}$  Single Crystals. *J. Appl. Phys.* 1968, 39, 2268-2274.

- (21) Ederer C.; Spaldin N. A. Weak Ferromagnetism and Magnetoelectric Coupling in Bismuth Ferrite. *Phys. Rev. B* 2005, 71, 060401(R).
- (22) Liu Z. Q.; Li L.; Gai Z.; Clarkson J. D.; Hsu S. L.; Wong A. T.; Fan L. S.; Lin M. -W.; Rouleau C. M.; Ward T. Z.; Lee H. N.; Sefat A. S.; Christen H. M.; Ramesh R. Full Electroresistance Modulation in a Mixed-Phase Metallic Alloy. *Phys. Rev. Lett.* 2016, 116, 097203.
- (23) Luo Y.; Pourovskii L.; Rowley S. E.; Li Y.; Feng C.; Georges A.; Dai J.; Cao G.; Xu Z.; Si Q.; Ong N. P. Heavy-fermion quantum criticality and destruction of the Kondo effect in a nickel oxypnictide. *Nat. Mater.* 2014, 13, 777-781.
- (24) Luo Y.; Ronning F.; Wakeham N.; Lu X.; Park T.; Xu Z. -A.; Thompson J. D. Pressure-tuned quantum criticality in the antiferromagnetic Kondo semimetal  $\text{CeNi}_{1.8}\text{As}_2$ . *Proc. Natl. Acad. Sci.* 2015, 112, 13520-13524.
- (25) Karthik J.; Damodaran A. R.; Marin L. W. Epitaxial Ferroelectric Heterostructures Fabricated by Selective Area Epitaxy of  $\text{SrRuO}_3$  Using an MgO Mask. *Adv. Mater.* 2012, 24, 1610-1615.
- (26) Dedon L. R.; Saremi S.; Chen Z.; Damodaran A. R.; Apgar B. A.; Gao R.; Martin L. W. Nonstoichiometry, Structure, and Properties of  $\text{BiFeO}_3$  Films. *Chem. Mater.* 2016, 28, 5952-5961.

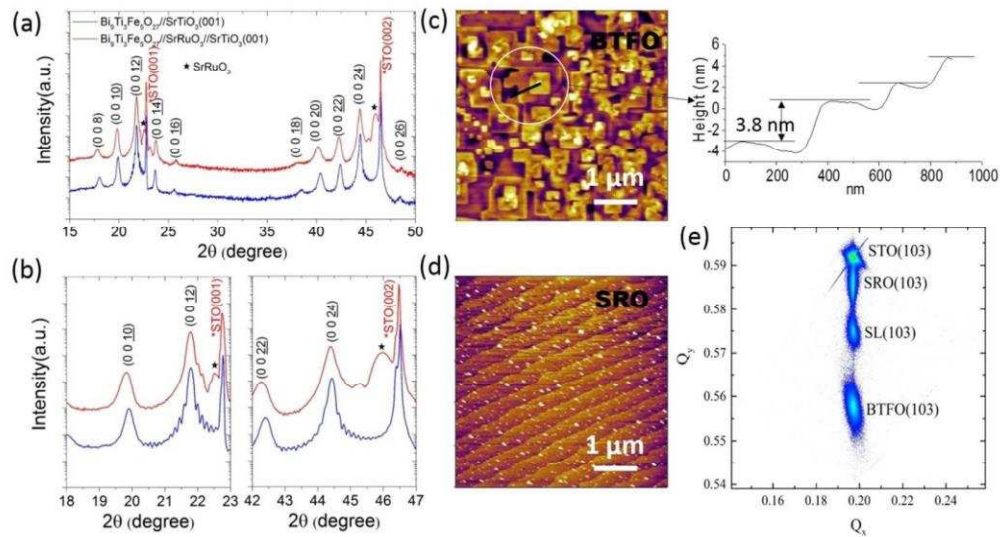


**Figure 1.** (a) and (b) are HRXRD  $\omega$ - $2\theta$  scans of BTFO/STO and BTFO/SRO/STO films, indicating a typical c-axis-oriented epitaxial Aurivillius oxide thin film. (c) Topography of the high-quality epitaxial BTFO thin film. The right panel shows an average step height with about 3.8 nm derived from the area. (d) Topography of the high-quality epitaxial SRO thin film. Obvious terraces were observed. (e) X-ray reciprocal space mapping around (103) STO, (103) SRO and (103) BTFO diffraction peaks.

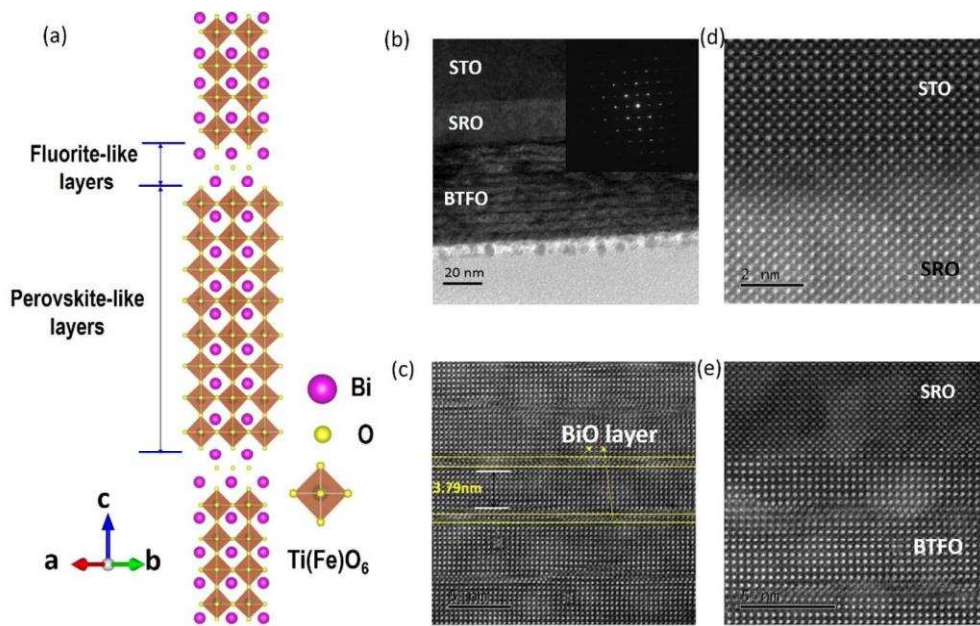


**Figure 2.** (a) Schematic diagram of the 8 layer Aurivillius BTFO film structure. (b) STEM of the BTFO/SRO/STO epitaxial thin film. Inset is the selected area electron diffraction (SAED) pattern of the BTFO/SRO/STO heterostructure. (c) Atomic-resolution HAADF-STEM image taken from cross-section of BTFO film. (d) and (e) Atomic-resolution HAADF-STEM image taken from the interfaces of STO/SRO and SRO/BTFO.

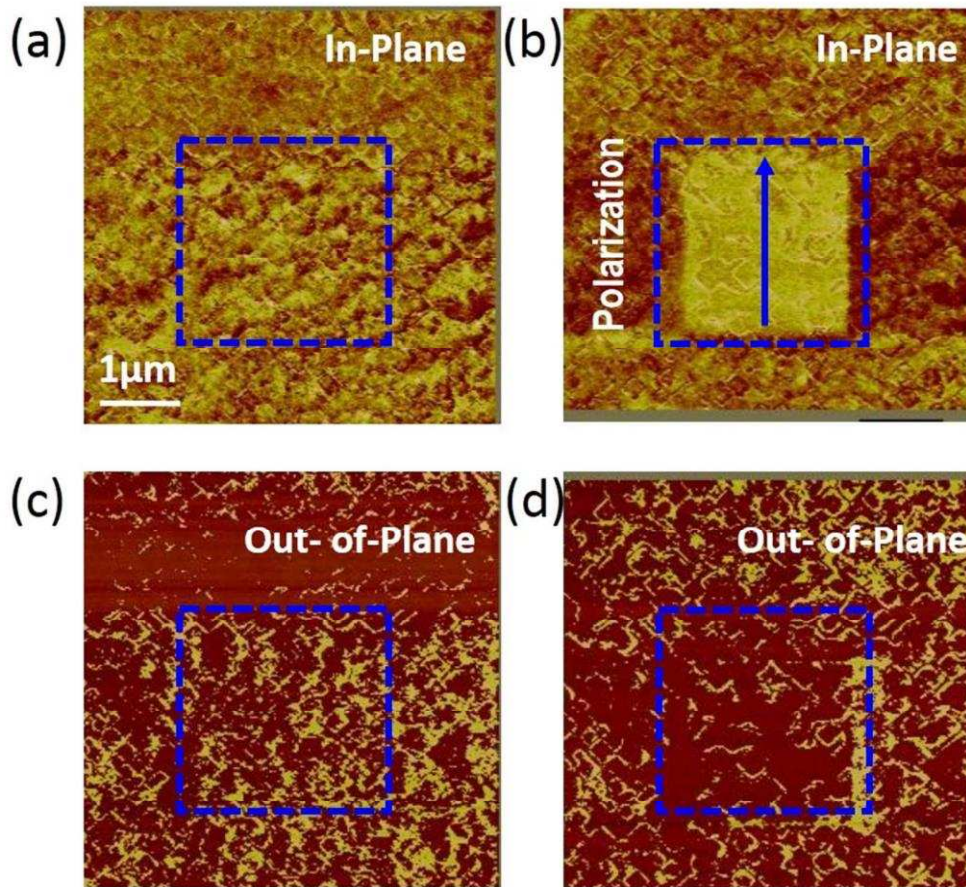


**Figure 3.** (a) and (b) PFM images of the BTFO film along in-plane direction before and after poling with +20 V voltage on the tip. Blue arrow represents polarization along in-plane direction. (c) and (d) PFM images of the BTFO film along out-of-plane direction before and after poling with +20 V voltage on the tip. All images were taken in an area of  $5 \times 5 \mu\text{m}^2$  and an applied dc bias of +20 V was written over a  $2 \times 2 \mu\text{m}^2$  area. All tests were carried out at room temperature.

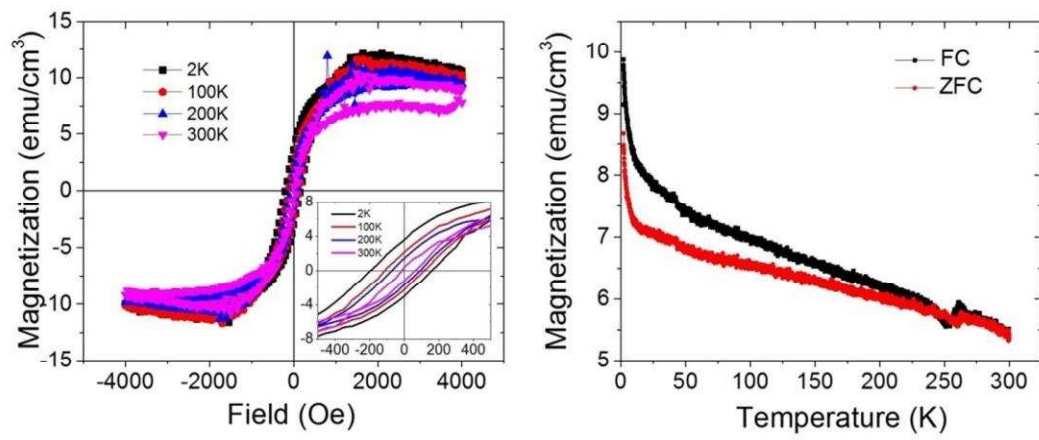


**Figure 4.** (a) In-plane magnetic hysteresis loops at different temperatures from 2K to 300 K. Inset shows an enlarged view of in-plane M-H loops of the BFTO film. (b) Temperature dependence of magnetization was obtained with an applied field of 1000 Oe. FC measurement was conducted with a cooling field of 1000 Oe.

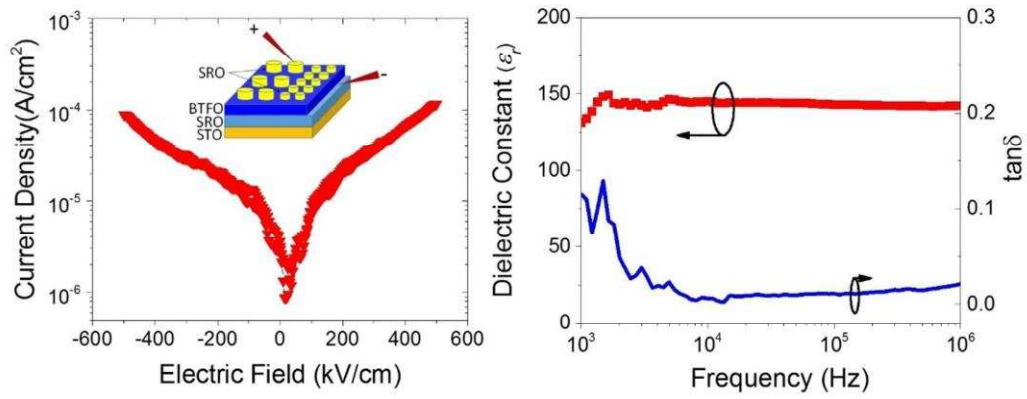


**Figure 5.** (a) Current-voltage (I-V) characteristic for a SRO/BTFO/SRO/STO heterostructure. The inset shows a schematic of the tested sandwiched structure of SRO/BTFO/SRO. (b) Dielectric constant and loss tangent of the BTFO film as a function of frequency. All the electrical measurements were carried out at room temperature.